Phase lagged coupled Kuramoto oscillators on Simplicial Complexes

Master Thesis

by

Bhuwan Moyal

(Roll No. 2103151005)

Under the Guidance of

Prof. Sarika Jalan

Department of Physics

Indian Institute of Technology Indore

07/06/2023

Certificate

I hereby certify that the work which is being presented in the thesis entitled **"Phase lagged Coupled Kuramoto Oscillators with higher-order interactions"** in the partial fulfilment of the requirements for the award of the degree of **Master of Science** and submitted in the **Discipline of Physics, Indian Institute of Technology Indore**, is an authentic record of my own work carried out during the time period from July 2022 to June 2023 under the supervision of **Prof. Sarika Jalan, Professor, Indian Institute of Technology Indore.** The matter presented in this thesis has not been submitted by me for the award of any other degree of this or any institute.

Bmoyal (07/06/2023)

Signature of the student with date
(Bhuwan Moyal)
07/06/2023

This is to certify that the above statement made by the candidate is correct to the best of my knowledge.

Signature of the Supervisor of M.Sc. thesis (with date)
(Prof. Sarika Jalan)
07/06/2023

Bhuwan Moyal has successfully given his M.Sc. Oral Examination held on 07th June, 2023.

Signature of Supervisor of M.Sc. thesis

Date: 07/06/2023

Convener, DPGC

Date: 13/6/2023

10.06.2023

Signature of PSPC Member no.1

Date:

Signature of PSPC Member no. 2

Date: 10.06.2023

Acknowledgements

It is important to acknowledge the support and contributions of individuals who have played a role in one's academic journey. I would like to express my gratitude towards my parents and elder sister for their constant encouragement and support. Additionally, I am grateful to my supervisor Prof. Sarika Jalan for her guidance and motivation during my time pursuing my MSc at IIT Indore.I would also like to extend my thanks to my PhD seniors Subha Sanket Dutta and Priyanka Rajwani and all the other members of the complex systems lab for having invaluable advice and discussions for my work. Special thanks go to my roommate Shankar for having engaging and insightful physics discussions and keeping me encouraged throughout the semester.

Abstract

The study of explosive synchronization in higher-order interactions has been of keen interest among many researchers. There have been several models for higher-order interactions, here we consider the 2-simplex $2\theta_i$ model with the phase lag parameter introduced to see how it affects the dynamics and thereby the critical coupling of the system. The present work is a generalization of the previous one where the study was limited to the case of vanishing α and symmetric distribution of ω_i. As in the previous case(Work which has already been done by Per Sebastion Skardal and Alex Arenas), a particular macroscopic solution of steady rotation is found, which branches off the trivial solution at some positive K. For pairwise Globally coupled networks with phase frustration work has been done by Sakaguchi and Kuramoto in 1986. Here we present an analysis of the collective dynamics of a 2-simplicial system with non-zero phase lag. In the later chapters, we also present the analytics of the $2\theta_j$ model in the presence of pair-wise interactions among the oscillators in which we see that along with the transition point nature of transition also changes on varying ϕ.

Contents

List of Figures

Symbols

r	Order parameter
θ_i	Phase of ith oscillator
K	Coupling interaction constant
ϕ	phase lag
ψ	mean phase

Chapter 1

Introduction

1.0.1 Complex systems

The concept of complexity is often regarded as a novel unifying framework for scientific inquiry, revolutionizing our comprehension of systems that have proven challenging to predict and control. Examples include the human brain and the global economy. One way to define a complex system is by its heightened sensitivity to initial conditions or small perturbations during evolution. Such systems possess a large number of independent interacting components or exhibit multiple pathways for evolution. Mathematical representations of these systems typically necessitate nonlinear differential equations. Another more subjective characterization deems a system "complicated" and resistant to precise description, whether analytical or otherwise.[8]

Complexity theory suggests that extensive collections of units have the capacity to autonomously organize into clusters that give rise to patterns, retain information, and participate in collective decision-making processes. A common thread throughout research on complexity involves systems comprising multiple elements that adapt and respond to the patterns emerging from these elements' interactions.

FIGURE 1.1: Flashing of fireflies

FIGURE 1.2: Flock of birds

1.0.2 Nonlinearity

Nonlinearity is often regarded as a fundamental characteristic of complexity. Linear systems exhibit superposition property, where adding any two solutions yields another solution, and scaling any solution by a factor produces another valid solution. However, nonlinearity disrupts this superposition principle. In many cases, we analyze systems by considering detailed states, such as the positions and momenta of particles, as inputs for dynamical equations, while our primary interest lies in coarse-grained physical quantities derived from these microstates. Nonlinear equations of motion can result in small variations in initial conditions leading to significantly different macrostates. These systems lack proportionality and straightforward causality between the stimuli's strength and the responses' magnitude. Small changes can produce unexpected and dramatic effects, while substantial stimuli do not always result in drastic changes in system behavior.[8]

1.0.3 Feedback

Feedback plays a crucial role as a necessary component in complex dynamical systems. In such systems, a part of the system receives feedback when its future interactions with neighboring components are influenced by its past interactions with them. Take, for example, a flock of birds. Each bird determines its course based on the positions and orientations of nearby birds. However, after adjusting its own trajectory, the bird's neighbors also modify their flight plans, partly in response to the first bird's new path. Consequently, when the bird considers its next move, the states of its neighbors now partially reflect its own earlier behavior.[8]

Feedback alone is not enough to manifest complexity in a system. It is crucial for individuals to be part of a sufficiently large group in order to exhibit complexity. Additionally, the feedback within the system must give rise to higher-level order. For instance, consider the behavior of ants. Individually, ants lack understanding of complex tasks such as building bridges or farms. However, when interacting with one another, they are able to undertake these intricate tasks. Left to their own devices, ants would exhibit simpler behavior. The emergence of complex behavior in ants is a result of their interactions and the feedback they exchange within the colony.[8]

1.0.4 Spontaneous Order

[8] The concept of order in the behavior of complex systems arises from the cumulative effect of numerous uncoordinated interactions between their elements. This fundamental idea is at the core of complex systems research. Related notions include symmetry, organization, periodicity, determinism, and pattern. It is worth noting that the term "order" encompasses various meanings, requiring careful qualification

for analytical usefulness in a theory of complex systems. However, it is evident that some notion of order is essential because pure randomness does not give rise to complexity. Conversely, total order is also incompatible with complexity. The fact that complex systems exhibit neither pure randomness nor complete order holds significant importance. Nevertheless, the existence of spontaneous order is a necessary condition for a system to be considered complex.

1.0.5 Robustness and lack of central control

The order observed in complex systems is characterized as robust due to its distributed nature, which means it is not centrally produced and remains stable even when the system is perturbed. For instance, the coordinated motion of a flock of birds persists despite its members' individual and erratic movements. This stability is demonstrated by the flock's ability to withstand external factors such as wind buffeting or random elimination of some flock members without losing its order. It is important to note that while the absence of central control is a common feature of complex systems, it is not sufficient for complexity, as non-complex systems may lack control or order altogether[8].

One mechanism through which a system can maintain its order is through the utilization of error-correction processes. Robustness is deemed necessary but not solely sufficient for complexity, as a random system can also be considered robust in the trivial sense that perturbations do not impact its order due to the absence of any inherent order. An example of robustness can be found in the climatic structure of the Earth's weather, where rough yet relatively stable regularities and periodicities in wind velocity, temperature, pressure, and humidity arise from underlying nonlinear dynamics. It is worth noting that these properties represent coarse-grained descriptions relative to the underlying state space. The existence of such properties enables a significant reduction in the number of degrees of freedom that need to be considered, forming an important area of study[8].

1.0.6 Emergence

When discussing complexity science, it is often associated with the limitations of reductionism. One prominent aspect of emergence is the notion of downward causation, which suggests that emergent objects, properties, or processes exert causal influence at higher levels of the organization. Upward causation, on the other hand, is widely accepted. For example, a subatomic decay event can generate radiation that induces a mutation in a cell, ultimately leading to the demise of an organism. The realms of biology, chemistry, economics, and social interactions are not causally isolated from physics, as physical causes can have effects in these domains. However, many hold the view that the physical world is causally closed, meaning that all physical effects have physical causes[8].

In the context of emergence, we are concerned with a specific type of emergence exemplified by phenomena such as the formation of crystals, the organization of ant colonies, and the emergence of higher levels of organization from fundamental physics and the physical components of complex systems. This notion of emergence is distinct from the emergence of approximately elliptical orbits over time through the gravitational interaction between the sun and the planets. The focus lies on understanding how levels of organization in nature emerge from the underlying principles of fundamental physics and the physical constituents of more complex systems[8].

1.0.7 Hierarchical organisation

Complex systems often exhibit multiple layers of organization, forming a hierarchical structure of systems and subsystems, as proposed by Herbert Simon in his influential paper "The Architecture of Complexity." These complex systems, characterized by various features mentioned earlier, give rise to entities with diverse levels of structure and properties. These levels interact with one another, displaying lawlike and causal regularities, as well as different forms of symmetry, order, and periodic behavior[8].

A prime example of such a system is an ecosystem, encompassing the entirety of life on Earth. Other examples of systems demonstrating this kind of organization include individual organisms, the brain, complex organisms' cells, and so forth. Even non-living entities, such as the cosmos exhibit this organizational structure, with atoms, molecules, gases, liquids, chemical and geological classifications, and ultimately stars, galaxies, clusters, and superclusters forming its intricate composition[8].

1.0.8 Vulnerability due to interconnectivity

Upon initial observation, the two satellite images of Image 1.1 appear identical, depicting illuminated regions in densely populated areas and darker regions representing extensive uninhabited forests and oceans. However, a closer examination reveals noticeable differences: (a) displays bright lights emanating from Toronto, Detroit, Cleveland, Columbus, and Long Island, whereas these areas appear dark in (b). These images depict the actual Northeast USA on August 14, 2003, before and after a significant blackout that left approximately 45 million people without power in eight US states, along with an additional 10 million in Ontario[7].

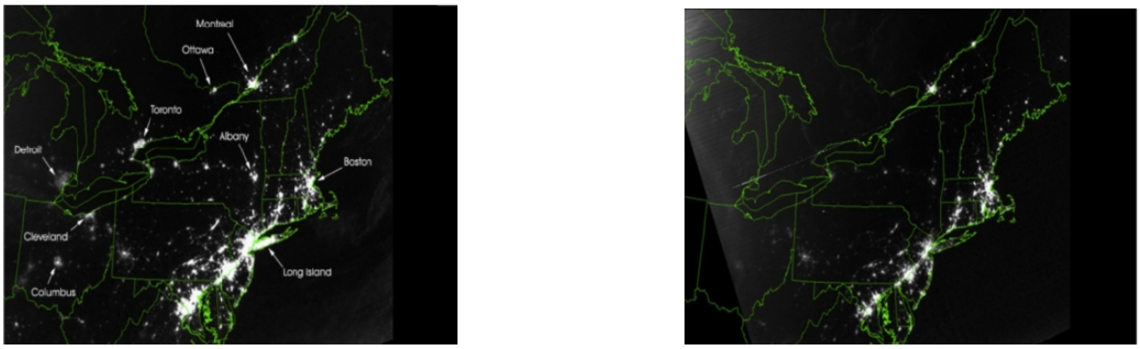

FIGURE 1.3: [7]Satellite image on the Northeast United States on August 13th, 2003, at 9:29 pm (EDT), 20 hours before the 2003 blackout. The same as above, but 5 hours after the blackout

The scenario described is a classic example of cascading failure. In a network functioning as a transportation system, when a local failure occurs, the load is shifted to other nodes within the system. If the additional load is manageable, the system can absorb it, and the failure goes unnoticed. However, if the neighboring nodes become overwhelmed by the increased load, they, too, will fail and redistribute the load to their own neighbors. This chain reaction results in a cascading event, the scale of which depends on the initial failed nodes' positions and capacities.

Cascading failures can also be intentionally induced. For instance, there is a global effort to disrupt the financial resources of terrorist organizations, with the goal of severely impeding their ability to operate effectively. Similarly, in the field of cancer research, scientists aim to trigger cascading failures within our cells to target and eliminate cancer cells.

During the initial stages of electric power generation, individual cities had their own generators and electric networks. Since electricity cannot be stored efficiently, it was necessary for it to be consumed immediately upon production. As a result, connecting neighboring cities and establishing a shared network became economically viable. This interconnectedness enabled the sharing of surplus electricity among cities and facilitated the borrowing of electricity when needed. The power grid, which emerged through these pairwise connections, played a crucial role in the affordability of electricity today. This extensive network links all electricity producers and consumers, allowing cheaply produced power to be efficiently transported to any location instantaneously. The domain of electricity serves as an excellent example of the significance of networks in our daily lives.

Chapter 2

General Definitions and Roadmap to Kuramoto Model

2.1 Networks and Graphs

[7]In order to comprehend a complex system, it is crucial to understand the interactions among its components. A network serves as a representation of a system's components, often referred to as nodes or vertices, along with the direct interactions between them, known as links or edges.

The size of the network, denoted as N, corresponds to the number of nodes or components within the system. To differentiate between nodes, we label them as i = 1, 2, ... N.

The total number of interactions between the nodes is referred to as the number of links, denoted as L. Links can be identified by the nodes they connect. For instance, a link between nodes 2 and 4 would be represented as (2, 4).

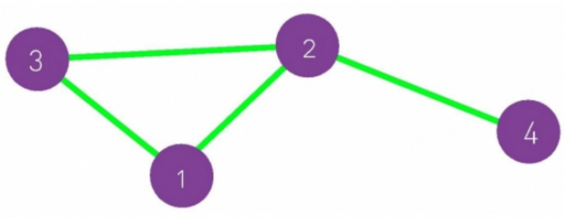

FIGURE 2.1: [7]

Networks can consist of either directed or undirected links. If all the links in a network are directed, it is termed a directed network or digraph. An example of a directed network is the World Wide Web (WWW), where uniform resource locators (URLs) point from one web document to another. On the other hand, if all the links are undirected, the network is called an undirected network. Some networks may contain a combination of directed and undirected links. For instance, in a metabolic network, certain reactions are reversible and can occur in both directions (undirected), while others only proceed in one specific direction (directed).

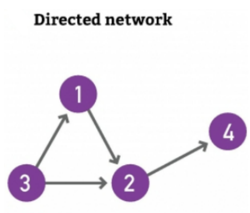

FIGURE 2.2: [7]

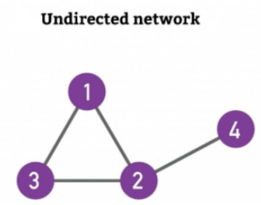

FIGURE 2.3: [7]

2.2 Degree, Average Degree, and Degree Distribution

[7]A crucial characteristic of each node in a network is its degree, which signifies the number of links it possesses connecting it to other nodes. The degree of a node can be interpreted as the number of mobile phone contacts an individual has in a call

graph, indicating the number of people the person has communicated with, or it can represent the number of citations a research paper receives in a citation network.

2.2.1 Degree

[7]The degree of the ith node in the network is denoted by "k." For instance, in the undirected networks depicted in the figure, the degrees of the nodes can be represented as k1=2, k2=3, k3=2, and k4=1. In the case of an undirected network, the total number of links, denoted as "l," can be calculated as the sum of the node degrees.:

$$L = \frac{1}{2}\sum_{i=1}^{N} k_i$$

The factor $\frac{1}{2}$ corrects for the fact that in the above sum, each link is counted twice.

2.2.2 Average Degree

[7]An important property of a network is its average degree, which for an undirected network is

$$\langle k \rangle = \frac{1}{N}\sum_{i=1}^{N} k_i = \frac{2L}{N}$$

In directed networks, a distinction is made between the incoming degree, denoted as k_i^{in}, which indicates the number of links directed towards node i, and the outgoing degree, denoted as k_i^{out}, which signifies the number of links originating from node i and pointing to other nodes. The total degree of a node, k_i, is the sum of its incoming and outgoing degrees.

$k_i = k_i^{in} + k_i^{out}$. For instance, in the World Wide Web (WWW), the outgoing degree (k_i^{out}) of a document corresponds to the number of pages it links to, while the incoming degree (k_i^{in}) represents the number of documents that link to it. The total number of links in a directed network can be expressed as the sum of the incoming degrees or the sum of the outgoing degrees:

$$L = \sum_{i=1}^{N} k_i^{in} = \sum_{i=1}^{N} k_i^{out}$$

In the case of directed networks, the factor $\frac{1}{2}$ is not present since the two sums in the equation are separately accounted for the incoming and outgoing degrees. The average degree of a directed network can be calculated by dividing the total number of links by the number of nodes.

$$\langle k \rangle = \frac{1}{N} \sum_{i=1}^{N} k_i^{in} = \frac{1}{N} \sum_{i=1}^{N} k_i^{out} = \frac{L}{N}$$

2.2.3 Degree Distribution

[7] The degree distribution, denoted as p_k, represents the probability that a randomly selected node in the network has a degree of k. To ensure that p_k is a valid probability distribution, it must be normalized, meaning that the sum of all probabilities must equal 1:

$$\sum_{k=1}^{\infty} p_k = 1$$

In a network with N nodes, the degree distribution can be expressed as the normalized histogram, given by: $p_k = \frac{N_k}{N}$ where N_k is the number of degree-k nodes. Hence the number of degree-k nodes can be obtained from the degree distribution as $N_k = Np_k$

$$A_{ij} = \begin{matrix} A_{11} & A_{12} & A_{13} & A_{14} \\ A_{21} & A_{22} & A_{23} & A_{24} \\ A_{31} & A_{32} & A_{33} & A_{34} \\ A_{41} & A_{42} & A_{43} & A_{44} \end{matrix}$$

FIGURE 2.4: Adjacency Matrix

2.2.4 Adjacency matrix

[7] To fully describe a network, it is necessary to have information about the links between its nodes. One way to keep track of these links is by providing a complete list of them. For instance, in the network depicted in the figure, we can uniquely describe it by listing its four links as follows: (1,2), (1,3), (2,3), (2,4).

In mathematical terms, networks are often represented using an adjacency matrix, particularly for directed networks consisting of N nodes. The adjacency matrix is an N x N matrix where each element represents the presence or absence of a link between nodes. Specifically:

If there is a link pointing from node j to node i, the corresponding element in the adjacency matrix, denoted as A_{ij}, is assigned a value of 1. If there is no link between the ith and jth node, the element A_{ij} is assigned a value of 0. By utilizing the adjacency matrix, we can efficiently represent the connectivity pattern of a network and analyze its properties and dynamics.

In the case of an undirected network, each link between nodes is represented by two entries in the adjacency matrix. For example, the link (1,2) is represented as $A_{12} = 1$ and $A_{21} = 1$. As a result, the adjacency matrix of an undirected network exhibits symmetry, meaning that $A_{ij} = A_{ji}$.

The degree of a node, denoted as k_i, can be determined directly from the elements of the adjacency matrix. In undirected networks, the degree of a node is calculated by summing either the corresponding row or column of the matrix:

$$k_i = \sum_{j=1}^{N} A_{ij} = \sum_{i=1}^{N} Aji$$

For the directed networks the sums over the adjacency matrix's rows and columns provide the incoming and outgoing degrees, respectively:

$$k_i^{in} = \sum_{j=1}^{N} A_{ij}, k_i^{out} = \sum_{i=1}^{N} Aji$$

2.2.5 Clustring Coefficients

[7] The clustering coefficient quantifies the extent to which the connections between neighbors of a specific node are interconnected. When considering a node i with a degree of k_i, the clustering coefficient is defined as a measure of this phenomenon.

$$C_i = \frac{2L_i}{(k_i)(k_i - 1)}$$

where L_i represents the number of links between the k_i neighbors of node i. The value of C_i is between 0 and 1:

$C_i = 0$ if none of the neighbors of node i link to each other. $C_i = 1$ if the neighbors of node i form a complete graph, that is they all are linked to each other.

So C_i basically measures the network's local density: the more is the density of inter-connected nodes in the neighborhood of node i, the higher its clustering coefficient.

2.3 Motivation for Kuramoto Model

[2]Our main focus to study this model was that for $N \to \infty$ we want to reduce the n dynamical equations into a single differential eq into single eq. involving the mean field parameters since we want to study the collective behavior of the system which can be done if we somehow are able to reduce the n differential equations into a single eq. involving variables that give us information about synchronization in the system, a system of oscillators spontaneously locks to a common frequency, despite having differences in the intrinsic frequencies of individual oscillators. There are various biological instances that exemplify the concept of clustering coefficients in networks. These include networks of pacemaker cells within the heart, circadian pacemaker cells found in the suprachiasmatic nucleus of the brain (where recent studies have successfully measured individual cellular frequencies), metabolic synchrony observed in yeast cell suspensions, gatherings of fireflies that synchronously flash, and groups of crickets that chirp in unison. Physics and engineering also provide numerous illustrations, ranging from arrays of lasers and microwave oscillators to superconducting Josephson junctions.

The mathematical study of collective synchronization originated with Wiener, who observed its presence in natural systems and proposed its potential involvement in generating alpha rhythms in the brain. However, Wiener's approach based on Fourier integrals ultimately proved to be a limited avenue of exploration.

In the first paper, Winfree introduced a more effective approach. He framed the problem in terms of a large population of interacting limit cycle oscillators. Recognizing the inherent complexity of the problem, Winfree hypothesized that simplifications could be achieved by weakening the coupling between oscillators and assuming their near-identical nature. Under these conditions, the oscillators would reach a steady state, converging to their limit cycles and becoming solely characterized by their evolving phases. These phases would be influenced by the interplay between weak coupling and variations in intrinsic frequencies among the oscillators.

To further streamline the model, Winfree proposed that each oscillator was coupled to the collective rhythm generated by the entire population, analogous to the mean-field approximation commonly employed in physics. His model incorporated these principles and paved the way for further advancements in the study of collective synchronization.

$$\dot{\theta}_i = \omega_i + (\sum_{j=1}^{N} P(\theta_J))Y(\theta_i)$$

for i=1,...,N, where θ_i denotes the phase of ith oscillator i and ω_i is its intrinsic natural frequency.Each jth oscillator exerts a phase-dependent influence P(θ_j) on all the others; the corresponding response of oscillator i depends on its phase θ_i, through the sensitivity function $Y(\theta_i)$.

Through a combination of numerical simulations and analytical approximations, Winfree made a significant discovery regarding populations of oscillators. He observed that these systems could demonstrate a temporal equivalent of a phase transition phenomenon. Specifically, when the range of natural frequencies among the oscillators was considerably larger than the strength of their coupling, the system exhibited incoherent behavior, with each oscillator operating independently at its intrinsic frequency.

However, as the range of natural frequencies decreased, the incoherence persisted until a critical threshold was surpassed. Beyond this threshold, certain oscillators began to synchronize, forming clusters of coherent behavior. Within these synchrony clusters, specific nodes or oscillators came together, displaying synchronized dynamics. This finding provided valuable insights into the emergence of synchronization in oscillator populations, shedding light on the conditions necessary for collective coherence.

2.4 Kuramoto Model

[2]The most successful attempt to explain synchronization was by Kuramoto in 1975, who analyzed a model of phase oscillators having arbitrary intrinsic frequencies and coupled through sine of their phase differences, locks to common frequency, despite the inevitable differences in the natural frequencies of individual oscillators. For weakly coupled, nearly identically limit-cycle oscillators, the governing equation for dynamics is given by

$$\dot{\theta}_i = \omega_i + \sum_{j=1}^{N} \lambda_{ij}(\theta_j - \theta_i)$$

for i=1,..,N The process of simplifying and analyzing the equations involved in the system is generally challenging due to the presence of numerous sinusoidal Fourier harmonics and the complexity arising from N equations representing the interconnected oscillators, which could be arranged in various topologies such as ring, chain, lattice, or other configurations. However, a more effective approach to represent these equations is through the mean-field approximation.

The Kuramoto model serves as the simplest case within this framework, where all oscillators are connected to each other with equal weights, and the interaction term is sinusoidal in nature. This formulation captures the essential dynamics of the system, allowing for a more tractable analysis and understanding of the collective behavior of the oscillator population. By employing the mean-field approximation in the Kuramoto model, researchers have made significant progress in studying synchronization phenomena, which is

$$\lambda_{ij}(\theta_j - \theta_i) = \frac{K}{N} sin(\theta_j - \theta_i)$$

for K¿=0 is the coupling strength which tells how strongly a node is connected to another node and how much the surrounding nodes are affecting its dynamics and we divide it by factor $\frac{1}{N}$ to ensure that our system is well behaved when N tends to ∞. The ω_i are the intrinsic frequencies distributed according to some probability density $g(\omega)$ and for simplicity, it was assumed to be unimodal and symmetric about its mean frequencies Ω, i.e, $g(\Omega+\omega) = g(\Omega-\omega)$ for all the ω, like gaussian or Lorentzian distribution. Since there is rotational symmetry in the model we can set mean frequency $\Omega = 0$ by doing the transformation $\theta_i \to \theta_i + \Omega t$ for all i, which is the same as going into the frame which is rotating with frequency Ω. So our governing equation becomes

$$\dot{\theta}_i = \omega_i + \frac{K}{N} \sum_{j=1}^{N} sin(\theta_j - \theta_i), \tag{2.1}$$

for i=1,...,N. This eq. remains invariant because it subtracts Ω form all the ω_i and shifts the mean of $g(\omega)$ to zero and this function $g(\omega)$ is well behaved between $(-\infty, \infty)$

2.4.1 Order parameter

Consider a unit complex circle, on its circumference all the the oscillators are revolving then the complex order parameter is defined as the centroid of the phases of all the oscillators where r(t) measures the magnitude of phase coherence it is basically a macroscopic quantity which tells us about how much the system is in synchrony by giving us the magnitude of collective rhythm and $\psi(t)$ measures the average phase.

$$re^{i\psi} = \frac{1}{N}\sum_{j=1}^{N} e^{i\theta_j} \tag{2.2}$$

For instance, if all the oscillators move in a single tight clump, we have r$\approx$ 1 and the system behaves like one big oscillator, and if the oscillators are scattered around the circle, then r$\approx$ 0, there is no coherence since each oscillator is incoherent and no rhythm is found. eq (2.1) can be written in the mean field by following by multiplying $e^{-i\theta_j}$ in eq. (2.2) We get

$$re^{\psi-\theta_i} = \frac{1}{N}\sum_{j=1}^{N} e^{i(\theta_j-\theta_i)}$$

Equating the imaginary parts we get

$$rsin(\psi-\theta_i) = \frac{1}{N}\sum_{j=1}^{N} sin(\theta_j-\theta_i)$$

. Thus (2.1) becomes

$$\dot{\theta}_i = \omega_i + Krsin(\psi-\theta_i) \tag{2.3}$$

for i=1,...,N The equation referred to as the mean field equation provides a more manageable framework for analysis. While it may initially appear that each oscillator is decoupled from the others, the oscillators actually interact through mean-field quantities represented by ψ and r. In this scenario, each oscillator aims to synchronize with the mean phase ψ rather than directly with other oscillators. Additionally, the effective strength of coupling is proportional to the value of r, leading to a positive feedback loop between coupling and coherence.

As the system becomes more coherent, r increases, causing the effective coupling strength, Kr, to grow as well. This heightened coupling strives to bring more oscillators into the synchronized cluster, initiating a feedback process. This positive feedback mechanism continues as r is further increased, promoting the expansion of the coherent cluster and enhancing synchronization within the oscillator population.

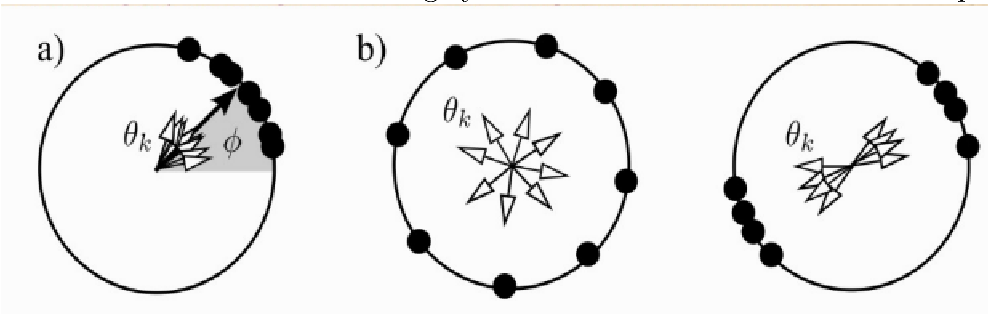

Here we can see that in (a) we notice a synchronized cluster where r is close to 1 and here ϕ is a mean phase of the cluster, distributed around ϕ in the same fashion as $g(\omega)$ distribution. In (b) r is close to zero in the first case as there is complete incoherence but in the second case although r is close to zero here also but here there is still cluster synchronization.

2.4.2 Analytics

Now if we go into the rotating frame rotating with Ω and we sit on the mean phase of the frame then we get

$$\dot{\theta}_i = \omega_i - krsin(\theta_i) \tag{2.4}$$

In steady-state solutions, the assumption of a constant value for r implies that all oscillators within the system appear to be independent. Consequently, solving for the resulting motions of the oscillators requires that the values of r and ψ remain consistent with their initially assumed values. This consistency ensures that the obtained solutions align with the original assumptions made.

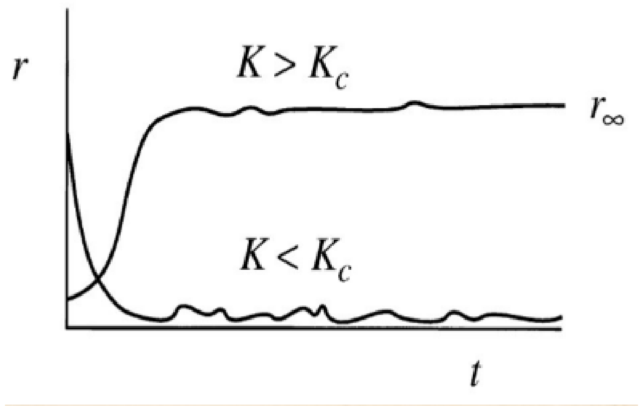

FIGURE 2.5: Evoution of r(t) seen from numerical simulations of r(t)[2]

The solutions exhibit two types of long-term behavior depending on the size of ω_i. The oscillators with —ω_i—¡= Kr approaches to a stable fixed point defined when $\dot{\theta}_i = 0$ then we get

$$\omega_i = krsin\theta_i$$

where $|\theta_i| <= \frac{\pi}{2}$. The mean field equation provides a convenient framework for analysis by considering the interaction between oscillators through mean-field quantities represented by ψ and r. While it may initially seem that each oscillator is independent, they actually synchronize with the mean phase ψ instead of directly interacting with other oscillators. The strength of coupling is determined by the value of r, creating a positive feedback loop between coupling and coherence.

As coherence increases, r also increases, leading to a growth in the effective coupling strength, Kr. This heightened coupling aims to bring more oscillators into the synchronized cluster, initiating a feedback process. This positive feedback mechanism continues as r further increases, promoting the expansion of the coherent cluster and enhancing synchronization within the oscillator population. Thus, the system evolves in a self-reinforcing manner, where increased coherence amplifies the coupling strength, fostering more extensive synchronization among the oscillators. So now the question arises that if all the drifting oscillators are buzzing around the circle in a nonuniform manner then how can r and ψ remain constant, this can only be true if the contributions of drifting oscillators even though moving in a nonuniform manner they should be uniformly distributed around the circle after reaching steady state which turns out to be true as we will see.

Let $\rho(\theta,\omega)d\theta$ denote the the fraction of oscillator distributed between θ to $\theta+d\theta$ at frequency ω. Now writing the continuity eq in (θ,ω) phase space

$$\frac{\partial\rho}{\partial t} = -\frac{\partial(\rho\dot{\theta})}{\partial\theta} \tag{2.5}$$

So the steady state means there is no piling or thinning of oscillators, we get

$$\rho(\theta,\omega) = \frac{C}{|\omega_i - Krsin(\theta)|} \tag{2.6}$$

The normalization constant is calculated by $\int_{-\pi}^{\pi}\rho(\theta,\omega)\,d\theta = 1$ for each ω, which gives $C = \frac{\sqrt{\omega^2-(Kr)^2}}{2\pi}$. Now self -consistency analysis the value of the order parameter must be consistent with (2.2) and by breaking down the averages in locked and drifting parts we get

$$r^{i\psi} = \langle e^{i\theta}\rangle_{lock} + \langle e^{i\theta}\rangle_{drift}$$

and since we are in the rotating frame so there $\psi = 0$ and in the locked state, for $|\omega| <= Kr$, $sin(\theta^*) = \frac{\omega}{Kr}$, for N $\to \infty$, the distribution of locked phases is symmetric about ψ and because of the symmetry of our distribution $g(\omega) = g(-\omega)$ so there will as many -θ^* as there are θ^* and so $\langle sin(\theta)\rangle_{lock}$ will cancel out and now if we see the contribution from the drifting oscillators we get

$$\langle e^{i\theta}\rangle_{drift} = \int_{-\pi}^{+\pi}\int_{|\omega|>Kr}\rho(\theta,\omega)e^{i\theta}\,d\omega\,d\theta$$

Now since due to the symmetry of $g(\omega)$ and from (2.6) it can be seen that $\rho(\theta, \omega) = \rho(\theta + \pi, -\omega)$ the above integral comes out to be zero so the self-consistency equation reduces to

$$r = Kr \int_{-Kr}^{Kr} cos(\theta) g(\omega)\, d\omega$$

changing variable in θ we get

$$r = Kr \int_{-\pi/2}^{\pi/2} cos^2(\theta) g(Krsin\theta)\, d\theta \tag{2.7}$$

Now there are two solutions to the above equations the trivial one is r=0 which means a completely incoherent state and so density will be $\rho(\theta, \omega) = \frac{1}{2\pi}$, and the other solution gives us the partially synchronized state which is given by the eq.

$$1 = K \int_{-\pi/2}^{\pi/2} cos^2(\theta) g(Krsin\theta)\, d\theta \tag{2.8}$$

and to calculate critical coupling strength we put $r \to 0^+$ in (2.8) and we get $K_c = \frac{2}{\pi g(0)}$. Now by doing the Taylor expansion of the integrand, we get

$$r \approx \sqrt{\frac{16}{\pi K_c^3}} \sqrt{\frac{\mu}{-g''(0)}} \tag{2.9}$$

where $\mu = \frac{K - K_c}{K_c}$ For the special case of Lorentzian distribution

$$g(\omega) = \frac{\gamma}{\pi(\gamma^2 + \omega^2)} \tag{2.10}$$

upon integrating (2.8) we get

$$r = \sqrt{1 - \frac{K}{K_c}} \tag{2.11}$$

for all $K >= K_c$

Chapter 3

Sakaguchi Kuramoto Model

3.1 Introduction

This model is a generalized version of the Kuramoto model with non-zero phase frustration in the system. This work was done by Sakaguchi and Kuramoto on April 17, 1986. Although the original work was done in the paper is done through the self-consistency method but we have done it here using the Ott-Antosen dimensionality reduction method and analytical progress is facilitated by the assumption that distribution describing the oscillator's natural frequencies take the form of Cauchy or Lorentzian Distribution. We show here that in addition to the low dimensional dynamics capturing fully the dynamics of the original system, the low dimensionality equations can be used to study the critical coupling strength corresponding to the onset of synchronization. These results agree with those which are obtained by a self-consistency framework, but by using Ott-Antosen ansatz the low dimensionality equations allow for a true bifurcation analysis that characterizes stability properties.

3.2 Analytics in thermodynamics limit

For Kuramoto Sakaguchi Model in the thermodynamic limit of infinitely many oscillators, relationships between r, Ω, coupling strength K and phase lag parameter can be found using the original self-consistency relation, but Ott-Antosen provides a simpler way of deriving the relationship for Lorentzian frequency distribution.

So our model equation is [1]

$$\dot{\theta}_i = \omega_i + \frac{K}{N}\sum_{j=1}^{N} sin(\theta_j - \theta_i - \phi) \tag{3.1}$$

for $|\phi| <= \frac{\pi}{2}$ where θ_j and θ_i are phases of ith and jth oscillator respectively and ω_i is frequency of ith oscillator and K¿=0 is the global coupling strength. The collective dynamics of this model i.e., the degree upto which the system will show synchronization and incoherence will depend mainly on the interplay of K, ω and ϕ if K is large enough with respect to spread and α, the system will synchronize.

Defining the complex order parameter

$$z = re^{i\psi} = \frac{1}{N}\sum_{j=1}^{N} e^{i\theta_j} \tag{3.2}$$

Now writing the eq(1) in terms of r and ψ we get by comparing the imaginary part of the above eq. and substituting in (1)

$$\dot{\theta}_i = \omega_i + Krsin(\psi - \theta_i) \tag{3.3}$$

We now discuss briefly of dimensionality of the reduction technique discovered by Ott Antonsen[4]. In the continuum limit where $N \to \infty$, we can describe the state of the system by density function $\rho(\omega, \theta, t)$, where $\rho(\omega, \theta, t)d\omega d\theta$ represents the probability or fraction of finding the oscillator having a frequency in between θ and $\theta + d\theta$ and having a frequency between ω to $\omega + d\omega$ at time t. First, we note that by conservation of oscillators, ρ must satisfy the continuity equation

$$\frac{\partial \rho}{\partial t} = -\frac{\partial(\rho\dot{\theta})}{\partial \theta} \tag{3.4}$$

which contains no $\partial/\partial\omega$ term since we have our natural frequencies to be fixed. Now also note that this function ρ is periodic in theta, so we Fourier expansion which takes the form

$$\rho(\theta, \omega, t) = \frac{g(\omega)}{2\pi}[\sum_{n=-\infty}^{\infty} \rho_n(\omega, t)e^{\iota n\theta} + c.c] \tag{3.5}$$

where ρ_n is the nth Fourier coefficient of the Fourier series and c.c. represents the complex conjugate of the previous term, so in this form determining the state of the Fourier coefficient ρ_n is equivalent to determining ρ. The main discovery of Ott-Antonsen is that all the Fourier coefficients collapse into one condition. By proposing that the Fourier coefficients decay geometrically, i.e., $\rho_n(\omega, t) = \alpha^n(\omega, t)$ for some function $\alpha(\omega, t)$ and so now substituting above equation in (3.4) and comparing the coefficients of $e^{in\theta}$, for different n the evolution of α and therefore distribution ρ can be calculated by single differential eq

$$\frac{\partial \alpha}{\partial t} + \iota\omega\alpha + \frac{K}{2}(z\alpha^2 e^{-\iota\phi} - z^* e\iota\phi) = 0 \tag{3.6}$$

where * represents the complex conjugate. To close the dynamics of the system we use that in the continuum limit we have

$$z(t)^* = \int\int \rho(\omega, \theta, t)e^{i\theta}\, d\theta\, d\omega \tag{3.7}$$

$$\int\int \frac{g(\omega)}{2\pi}[1+\sum_{n=1}^{\infty}[\bar{\alpha^n}(\omega,t)e^{-\iota n\theta}+\alpha^n(\omega,t)e^{\iota n\theta}]]e^{-\iota\theta}\,d\theta\,d\omega$$
$$=\int \alpha(\omega,t)g(\omega)\,d\omega$$

Integrating this in the lower half of the complex plane using Cauchy's integral theorem with a pole at $\omega = -\iota\triangle$ we get $z^* = \alpha(\omega_0 - \iota\triangle, t)$, here we consider our frequency distribution to be

$$g(\omega) = \frac{\triangle}{\pi[(\omega-\omega_0)^2+\triangle^2]} \tag{3.8}$$

with mean ω_0 and spread $\triangle > 0$. We note that by entering into the rotating frame we can set the mean to be zero without any loss of generality. At $\omega = -\iota\triangle$ we get

$$\dot{z^*} = -z^* + \frac{1}{2}[Kz^*e^{\iota\phi} - z^*z^*Kze^{-\iota\phi}]$$

Taking complex conjugate both sides we get

$$\dot{z} = \triangle z + \frac{1}{2}[Kze^{-\iota\phi} - z^2Kz^*e^{\iota\phi}] \tag{3.9}$$

Now by polar decomposition $z = re^{i\psi}$ substituting in (3.9) we get

$$\dot{r} = -\frac{1}{2}r[r^2Kcos(\phi) - 1 + \frac{2\triangle}{Kcos(\phi)}] \tag{3.10}$$

$$r\dot{\psi} = -\frac{1}{2}Krsin\phi(1+r^2) \tag{3.11}$$

Here the stable steady solution is r=0 for $0 < K < K_c$ is obtained where

$$K_c = \frac{2\triangle}{cos\phi} \tag{3.12}$$

For $K >= K_c$, we get pair of stable steady-state solutions

$$r = \pm\sqrt{1 - \frac{2\triangle}{K cos\phi}} = \pm\sqrt{1 - \frac{K_c}{K}} \tag{3.13}$$

which emerges through a supercritical pitchfork bifurcation at $K = K_c$. The positive solution corresponds to the partially synchronized state. Substituting this positive solution into (3.11) we get mean cluster frequency.

$$\Omega = \dot{\psi} = \triangle tan\phi - K sin\phi \tag{3.14}$$

As seen from the eq.(3.12) critical coupling is shifted towards the right as $\phi \in (0, \frac{\pi}{2})$ as the inclusion of ϕ causes frustration in the system, so the onset of synchronization at larger K_c and we see a continuous second order transition

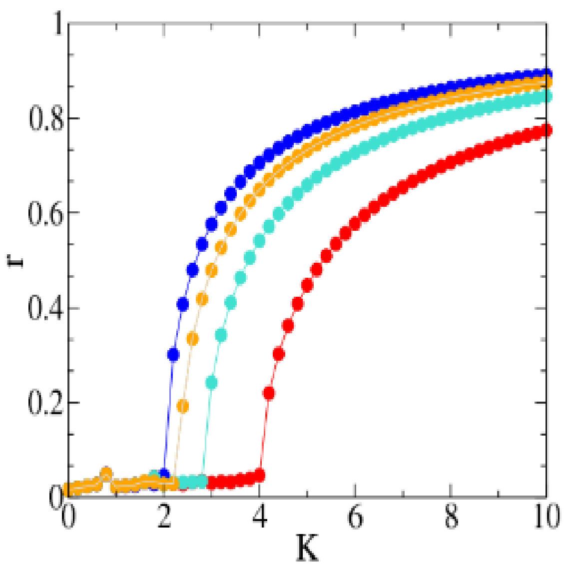

.

It can be seen here that as predicted by eq(3.2) value for critical coupling strength shifts towards the right causing frustration in the system. Here blue curve represents for ϕ=0 yellow for ϕ=pi/6, green for pi/4 and red for $\pi/3$

Chapter 4

Phase lagged coupled Kuramoto oscillators on Simplicial Complexes

4.1 Introduction

Here we present the generalized version of the Higher-order interactions mainly 3-way, 2 simplex, where n-simplex represents the interaction between n+1 units, so 2-simplices represent 3-way interaction. This work is a generalization of work which was done by Skardal and Alex Arenas on Abrupt Desynchronization and Extensive Multistability in Globally coupled Oscillator Simplices[9]. Here we have introduced a phase frustration parameter in the original eq to understand the dynamics. In particular the 2-simplex macroscopic dynamics are captured by a combination two order parameters namely r_1 and r_2 that tell the degree of synchronization and extent of asymmetry as the oscillators organize into two different synchronised clusters.

4.2 Model representation and Analytical derivation

We consider the dynamical equation as an extension of the Kuramoto Sakaguchi model [**kuramoto1975international**] with simplicial complexes, in particular, higher order (2-simplex) interactions such as

$$\dot{\theta}_i = \omega_i + \frac{K_2}{N^2} \sum_{j=1}^{N} \sum_{k=1}^{N} \sin(\theta_j + \theta_k - 2\theta_i - \phi). \tag{4.1}$$

Where ϕ is the phase lag between oscillators and K_2 is the 2-simplex coupling strength for N number of oscillators. To analyze the collective behavior of oscillators we introduce the definition of the generalized order parameter $z_q = r_q e^{\iota\psi_q} = \frac{1}{N}\sum_{j=1}^{N} e^{q\iota\phi_j}$, for (q=1,2), z_1 measures the extent of global synchronization and z_2 measures the clustering. This helps to write Eq. 4.1 into the mean field equation such as

$$\dot{\theta}_i = \omega_i + K_2 r_1^2 \sin(2\psi_1 - 2\theta_i - \phi), \tag{4.2}$$

where ψ_n is the generalized mean phase of oscillators given by equation

$$\psi_n = arctan \frac{(\sum_{j=1}^{N} sin(n\theta_j))}{(\sum_{j=1}^{N} cos(n\theta_j))} \tag{4.3}$$

In the continuum limit $N \to \infty$[3] the state of the system can be described by density function $\rho(\theta, \omega, t)$ i.e. the density of oscillators with phase between θ and $\theta + \delta\theta$ and intrinsic frequencies between ω and $\omega + \delta\omega$ at time t, since the number of oscillators is conserved in the system, ρ must satisfy the continuity equation

$$\frac{\partial \rho}{\partial t} = -\frac{\partial(\rho\dot{\theta})}{\partial\theta}. \tag{4.4}$$

Considering the frequency of each oscillator is drawn from the distribution $g(\omega)$ the density function is expanded into Fourier series

$$\rho(\theta, \omega, t) = \frac{g(\omega)}{2\pi}[\sum_{n=-\infty}^{\infty} \rho_n(\omega, t)e^{\iota n\theta}],$$

where $\rho_n(\omega, t)$ being the n^{th} Fourier coefficient and $\rho_{-n} = \rho_n^* e^{-\iota n\theta}$. We can write the density function into the sum of the symmetric and antisymmetric parts thus symmetric and antisymmetric parts satisfy $\rho(\theta + \pi, \omega, t) = \rho_s(\theta, \omega, t)$ and $\rho_a(\theta + \pi, \omega, t) = -\rho_a(\theta, \omega, t)$, respectively. The linearity property of the continuity equation defines that individually ρ_s and ρ_a are solutions therefore combination of both is also a solution. However, only the symmetric part allows for dimensionality reduction using Ott-Antonsen ansatz that all the Fourier modes decay geometrically because an asymmetric part on comparing coefficients for different α equations falls on different manifolds, i.e. $\rho_{2n}(\omega, t) = \alpha^n(\omega, t)$ where $|\alpha(\omega, t)| \leq 1$,

$$\rho_s(\theta, \omega, t) = \frac{g(\omega)}{2\pi}[1 + \sum_{m=1}^{\infty} \rho_{2n}(\omega, t)e^{in\theta} + c.c]. \tag{4.5}$$

plugging this and Eq. 5.2 into the continuity Eq. 4.4, We found that each subspace spanned by even terms $e^{2\iota n\theta}$ collapse into a one-dimensional manifold given by[5],

$$\frac{\partial \alpha}{\partial t} = -2\iota\alpha\omega + K_2(z_1^{*2}e^{\iota\phi} - z_1^2\alpha^2 e^{-\iota\phi}). \tag{4.6}$$

In the continuum limit $N \to \infty$, we have $z_2 = \int_{-\infty}^{\infty}\int_0^{2\pi} \rho_s(\theta, \omega, t)e^{\iota 2\theta} g(\omega) d\theta d\omega$, which after inserting the Fourier series expansion of $\rho_s(\theta, \omega, t)$ this reduces to $z_2 = \int_{-\infty}^{\infty} g(\omega)\alpha^* d\omega$. If we consider the frequency distribution $g(\omega)$ to be Lorentzian $g(\omega) = \frac{\Delta}{\pi[(\omega-\omega_0)^2+\Delta^2]}$ with mean $\omega_0 = 0$ and spread $\Delta = 1$, the integral z_2 can be calculated using Cauchy's Residue Theorem by contour integration in the negative half-plane, yielding $z_2 = \alpha^*(\omega_0 - \iota\Delta, t)$. After making this substitution and separating the real and imaginary parts, Eq. 4.6 reduces to

$$\dot{r_2} = -2r_2 + K_2{r_1}^2(1 - r_2^2)\cos(2\psi_1 - \psi_2 - \phi). \tag{4.7}$$

$$\dot{\psi}_2 = K_2 r_1^2 \frac{1 + r_2^2}{r_2} \sin(2\psi_1 - \psi_2 - \phi). \tag{4.8}$$

Although, these equations explain only the contribution of the symmetric part of the ρ_s, and indicate that it depends on the asymmetry part also as the information of r_1 is present in the evolution of equation of r_2 Eq. 4.7.
Proceeding further to analyze the z_1 using the self-consistency method. We change the frame of reference $\theta \rightarrow \theta + \psi$ and enter into the rotating frame where $(\dot{\psi} = \Omega)$ and setting ψ_1 and ψ_2 equal to zero. For $K > K_c$ some parts of oscillators form a synchronized cluster that evolves at some common non-zero frequency. We calculate the effective cluster frequency of $\Omega_i = \langle \dot{\theta}_i(t) \rangle_t$ for each oscillator where $\dot{\theta}_i(t)$ are instantaneous frequencies of those oscillators that take part in synchronized cluster C, at time t. Oscillators that take part in clusters are distributed in the complex circle around the mean ψ in the same manner as g(ω) distribution which has oscillators at the ends with minimal and maximal frequency and whenever there will be cutoff or addition of new oscillators on changing K it will not be in a symmetric manner, so the common frequency of cluster is calculated as $\Omega = \frac{1}{N_c} \sum_{j \in C} \Omega_j$, where $N_c = i_{max} - imin + 1$ denotes the size of the synchronized cluster. In the original model of Kuramoto with zero phase frustration $\phi = 0$, the synchronized cluster remains stationary if the mean of the frequency distribution is set to be zero and will be symmetric about $\omega = 0$ at all times. So $\omega_{max} = -\omega_{min}$ and we decrease the coupling strength the range of oscillators in the cluster decreases symmetrically whereas for non-zero phase frustration ϕ where the synchronized cluster is not symmetric about $\omega = 0$ and breaks off asymmetrically from the cluster.

For non-zero ϕ synchronized cluster moves with non-zero frequency in the ground frame even though the mean of our $g(\omega)$ was taken to be zero, asymmetry in instantaneous frequency is produced due to this phase lag parameterϕ whereas for $\phi = 0$ cluster remains stationary as the introduction of ϕ causes the cluster to move uniform non-zero frequency

Hence, Eq.5.2 can be written as

$$\dot{\theta}_i = \omega_i - \Omega - K_2{r_1}^2 \sin(2\theta + \phi) \tag{4.9}$$

Now, based on the dynamical behavior of oscillators the whole population can be divided into two groups of locked and drift oscillators such as $|s| \leq 1$ and $|s| > 1$, respectively, where ($a = K_2{r_1}^2$ and $s = \frac{\omega - \Omega}{a}$). Moreover, in the case of a locked state higher order coupling term shows the existence of two stable fixed points $\theta^* = \frac{1}{2}\arcsin(s) - \frac{\phi}{2}$ and $\theta^* + \pi$. First, to study the contribution of the locked oscillator population we can define the density function such as

$$\rho_{loc}(\theta, \omega) = \eta\delta(\theta - \theta^*) + (1 - \eta)\delta(\theta - (\theta^* + \pi)). \tag{4.10}$$

where η and $1 - \eta$ is the probability of number of oscillators at θ^* and $\theta^* + \pi$, respectively. Furthermore, the definition of $z_1 = \int_{-\infty}^{\infty} \int_0^{2\pi} e^{\iota\theta} \rho_{loc}(\theta, \omega) g(\omega) d\theta d\omega$ defines the contribution from locked oscillators given by,

$${r_1}^{lock} = (2\eta - 1) \int_{-a+\Omega}^{a+\Omega} e^{\iota\theta} g(\omega) d(\omega). \tag{4.11}$$

Moreover, for the locked state $\dot{\theta} = 0$ from Eq. 4.9

$$\sin(2\theta^* + \phi) = s \quad and \quad \cos(2\theta^* + \phi) = \sqrt{1 - s^2}.$$

using the trigonometric identities above equation can be expressed as

$$\begin{aligned} \cos(\theta^* + \frac{\phi}{2}) &= \sqrt{\frac{1+\sqrt{1-s^2}}{2}}, \\ \sin(\theta^* + \frac{\phi}{2}) &= \pm\sqrt{\frac{1-\sqrt{1-s^2}}{2}}, \end{aligned} \tag{4.12}$$

Considering, $\theta^* = \Theta - \frac{\phi}{2}$. Moreover, the contribution of sine term positive or negative determines based on limits of integration over ω. Hence, Eq. 4.11 can be expressed as

$$r_1{}^{lock} e^{\iota \frac{\phi}{2}} = \int_{-a+\Omega}^{a+\Omega} e^{\iota \theta^*} g(\omega) d\omega. \tag{4.13}$$

By plugging the value of Θ and comparing real and imaginary parts contribution from locked oscillators determined as

$$\begin{aligned} r_1{}^{lock} = (2\eta - 1)[\cos\frac{\phi}{2} &\int_{-a+\Omega}^{a+\Omega} \sqrt{\frac{1+\sqrt{1-s^2}}{2}} g(\omega) d\omega \\ &- \sin\frac{\phi}{2} \int_{-a+\Omega}^{\Omega} \sqrt{\frac{1-\sqrt{1-s^2}}{2}} g(\omega) d\omega \\ &+ \sin\frac{\phi}{2} \int_{\Omega}^{a+\Omega} \sqrt{\frac{1-\sqrt{1-s^2}}{2}} g(\omega) d\omega]. \end{aligned} \tag{4.14}$$

In addition, to analyze the contribution of drift oscillator population

$$r_1{}^{drift} = \int_{|\omega-\Omega|>a} \int_0^{2\pi} e^{\iota\theta} \rho_d(\theta,\omega) g(\omega) d(\omega) d(\theta). \tag{4.15}$$

from Eq. 4.4 in the steady state $\rho\dot{\theta}$ is constant which gives $\rho_d = \frac{C}{\dot{\theta}}$ and after normalization reduces into

$$\rho_d = \frac{\sqrt{(\omega-\Omega)^2 - a^2}}{2\pi|\omega - \Omega - a\sin(2\theta+\phi)|}$$

Now it can be seen that $\rho(\theta,\omega) = \rho(\theta+\pi,\omega)$. And by following property that $e^{i\theta} = -e^{i(\theta+\pi)}$ so rewriting the integral in θ we get

$$\int_0^{2\pi} e^{\iota\theta}\rho_d(\theta,\omega)g(\omega)d(\theta) = \int_0^{\pi}[e^{\iota\theta}\rho_d(\theta,\omega)g(\omega)d(\theta) + e^{\iota\theta}\rho_d(\theta=\pi,\omega)]g(\omega)d(\theta)$$

as now we can see that this integral vanishes due to symmetry of density function in θ.

(Eq. 4.15) $r_1 = r_1^{loc} + r_1^{drift} \approx r_1^{loc}$ given by Eq. 4.14.

Now Ω can be calculated using $\dot{\psi}_2$ eq(4.7). Recall that we calculate ψ in the (4.3), now in that equation, that sum in numerator and denominator can be broken into two parts, first is for synchronized cluster and the other is for drifting oscillators, and since we know that drifting oscillators does not contribute so that second part of sum contributes to zero in both num. and denom. so, only oscillators that take part in the cluster will contribute in $\psi 1$ and so we can say this ψ_1 is the mean phase of the cluster and similarly, we can calculate ψ_2 and here also it will mean of synchronized clusters only and it turns out that from (4.3) when $N \to \infty$ the sum becomes

$$\psi_n = arctan\frac{\int_{\theta_1}^{\theta_2} sin(n\theta_j)d\theta}{\int_{\theta_1}^{\theta_2} cos(n\theta_j)d\theta} \tag{4.16}$$

where θ_1 and θ_2 are end points of the cluster at time t. which upon solving gives $\psi_2 = 2\psi_1$ and so $\dot{\psi}_1$ can be calculated by using the relation (4.8) and the relation between r_1 and r_2 calculated at steady state

$$r_2 = \frac{-1+\sqrt{1+K^2r_1^4cos(\phi)^2}}{Kr_1^2cos(\phi)} \tag{4.17}$$

we can find $\dot{\psi}_1$ which is same as Ω for the synchronized cluster is written as

$$\dot{\psi}_1 = \Omega = (\sqrt{1 + K^2 r_1^4 cos\phi^2}) tan(\phi) \tag{4.18}$$

Now here for the forward process as we increase K no synchronization is seen because as $r_1 \to 0^+$ and $r_2 \to 0^+$, it comes out critical coupling goes to ∞ which can be seen from relation (4.16) if we invert it we get

$$K = \frac{2r_2}{(1 - r_2^2) cos\phi (r_1^2)}$$

from this we can see the denominator goes to zero at a much faster rate due to higher order polynomials so K goes to ∞.

Here we can see that at $K = K_c$ we see a saddle-node bifurcation from which one stable and other unstable branch is obtained, beyond which multistability is seen here in the thermodynamic limit, here we have drawn only four of them and we see a first-order backward transition. Here the value of r_2 will be greater than that of r_1 and it will be much more clearly shown as we decrease the η because then we are going toward the state of a system where the oscillators are going toward a state where there is symmetric distribution among two clusters and so r_1 will start decreasing relative to r_2. Here to calculate backward critical coupling strength we put $dk/dr_1 = 0$ from (4.14) and check for what particular values of K and r_1 (4.14) will be true.

Interpreting the analytical results with reference to numerical simulations we see that, partially synchronized branches are recognized by asymmetry parameter η, which indicates that the complexity of these dynamics arises from the allocation of locked oscillators in two different clusters but here we see that introducing ϕ causes frustration in r_2 also which means that if we do not want to change the distribution of

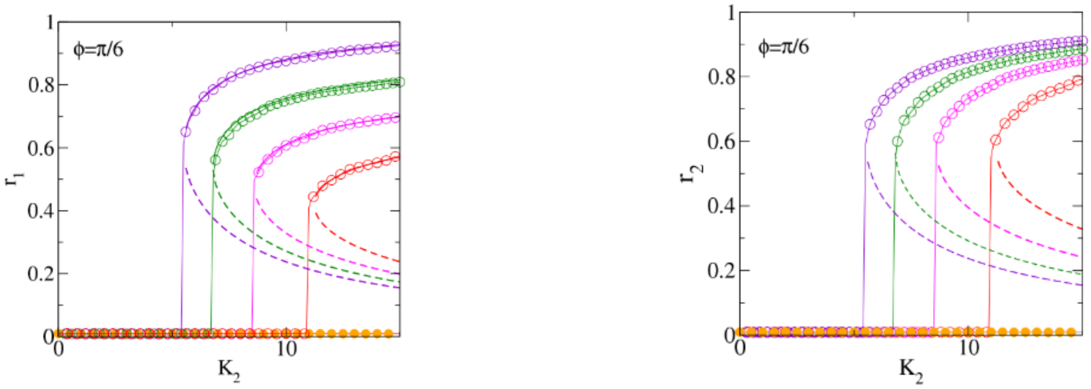

FIGURE 4.1: For fixed ϕ and varying η we see that on decreasing η, K_c shifts towards right, η=1 is the purple curve, η=0.95 is the green curve, η=0.9 is for pink curve and η=0.85 is the orange curve.

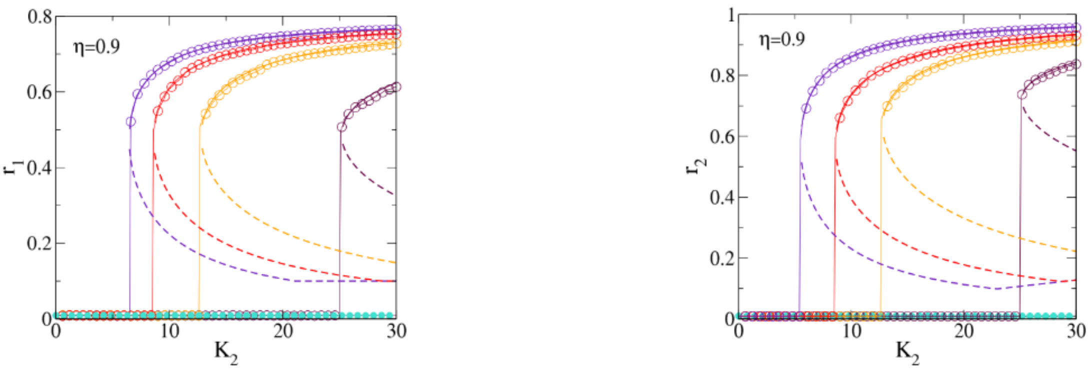

FIGURE 4.2: Here we fix η and increase ϕ, upon doing so we see that ϕ introduces frustration in the system causing the critical coupling to increase. the purple curve represents for $\phi = 0$, red curve is for $\phi = \pi/6$, yellow curve is for $\phi = \pi/4$, brown curve represents the $\phi = \pi/3$

the oscillators in the system and still wants to change the point of desynchronization so that can be achieved by introducing ϕ in the system.

So we see that upon introducing ϕ there was frustration caused in the system but here for r_2 also introducing ϕ has the same effect which means that the system will start diffusing from two clusters states and slowly going towards completely incoherent states(Have to check for three, four cluster states and so on), so a type of synchronized disorder can be achieved means that there can be many clusters possible distributed uniformly around the circle. So if we take our system with the mean of intrinsic frequencies distribution to be zero and we want that synchronized cluster to rotate with no zero frequency one way of doing this is that we can include the phase lag parameter. Its application can be found in glassy states and super relaxation and can be found wherever there is symmetry is broken in a frequency distribution. This model gives us much more insight into how microscopic frustration is caused in the system by accounting for two cluster states in the system. ref

Chapter 5

2-Simplex model with Pairwise interaction term

5.1 Introduction

Here we take a somewhat different model with pair-wise interacting term with phase frustration in the system.[10]

$$\dot{\theta}_i = \omega_i + \frac{K1}{N}\sum_{j=1}^{N} sin(\theta_j - \theta_i - \phi) + \frac{K_2}{N^2}\sum_{j=1}^{N}\sum_{k=1}^{N}\sin(2\theta_j - \theta_k - \theta_i - \phi). \tag{5.1}$$

Defining the generalized order parameter $z_q = r_q e^{\iota\psi_q} = \frac{1}{N}\sum_{j=1}^{N} e^{q\iota\phi_j}$, for (q=1,2). Using these definitions of order parameters we write our model equation in the mean-field we get

$$\dot{\theta}_i = \omega_i + K_1 r_1 sin(\psi_1 - \theta_i - \alpha) + K_2 r_1^2 \sin(\psi_2 - \psi - 2\theta_i - \phi), \tag{5.2}$$

Defining the usual density function

$$\rho(\theta, \omega, t) = \frac{g(\omega)}{2\pi}[1 + \sum_{n=1}^{\infty} \rho_n(\omega, t)e^{\iota n\theta}] \tag{5.3}$$

By Ott-Antonsen ansatz, the Fourier coefficients decay geometrically as $\rho_n(\omega, t) = \alpha^n(\omega, t)$ where $|\alpha| <= 1$ Since by conservation of oscillator,s ρ must satisfy the following equation[6]

$$\frac{\partial \rho}{\partial t} = -\frac{\partial(\rho\dot{\theta})}{\partial \theta}. \tag{5.4}$$

substituting ρ from (5.3) into the above equation and comparing the coefficients of $e^{i\theta}$ on both sides we get a single differential equation in α we get

$$\dot{\alpha} = -i\omega\alpha + \frac{K_1 r_1}{2}e^{-i(\psi_1-\phi)} + \frac{K_2 r_1 r_2}{2}e^{-i(\psi_2-\psi_1-\phi)} - \frac{K_1 r_1 \alpha^2}{2}e^{i(\psi_1-\alpha)} - \frac{K_2 r_1 r_2 \alpha^2}{2}e^{i(\psi_2-\psi_1-\alpha)}$$

In the continuum limit $N \to \infty$, we have $z_1 = \int_{-\infty}^{\infty}\int_0^{2\pi} \rho_s(\theta, \omega, t)e^{\iota\theta}g(\omega)d\theta d\omega$, which after inserting the Fourier series expansion of $\rho_s(\theta, \omega, t)$ this reduces to $z_1 = \int_{-\infty}^{\infty} g(\omega)\alpha^* d\omega$. and $z_2 = \int_{-\infty}^{\infty}\int_0^{2\pi} \rho_s(\theta, \omega, t)e^{\iota 2\theta}g(\omega)d\theta d\omega$, which after inserting the Fourier series expansion of $\rho_s(\theta, \omega, t)$ this reduces to $z_2 = \int_{-\infty}^{\infty} g(\omega)\alpha^* d\omega$. Here we take Cauchy distribution $g(\omega) = \frac{1}{\pi[\omega^2+1]}$ with mean 0 and spread 1 since this eq. has two poles so taking the lower half of the complex plane. integral of z_1 and z_2 can be calculated by closing the integration along the semicircle of infinite radius we get for $\omega = -iz_1 = \alpha^*$ and $z_2 = \alpha^{*2}$ and with the definition of z_1 and z_2 we get

$$\dot{r_1} = -r_1 - \frac{K_1}{2}r_1^3 cos\phi + \frac{K_1 r_1 cos\phi}{2} + \frac{K_2 r_1^3 cos\phi}{2} - \frac{K_2 {r_1}^5 cos\phi}{2} \tag{5.5}$$

and

$$\dot{\psi} = -\frac{1}{2}[r_1^2(K_1 + K_2{r_1}^2)sin\phi + (K_1 + K_2 r_1^2)sin\phi] \tag{5.6}$$

To calculate the now fixed point of (5.5) the long-term macroscopic state is given by

$$r_1 = \sqrt{\frac{(K_2 - K_1)cos\phi \pm \sqrt{(K_2 - K_1)^2 cos^2(\phi) - 8K_2 cos\phi}}{2K_2 cos\phi}} \tag{5.7}$$

. In order to calculate the point of saddle-node bifurcation we need to calculate the point of saddle-node bifurcation which occurs when r^+ and r^- tend to zero which gives the following relation

$$(K_1 + K_2)^2 cos\phi = 8K_2 \tag{5.8}$$

Now for the fixed value of K_1 and changing ϕ, the system goes from continuous transition to abrupt transition states. To check the stability for a trivial fixed point which will depend on if ϕ¡ cos(inv)($\frac{2}{K_1}$)then it will be unstable and stable if ϕ¿cos(inv)($\frac{2}{K_1}$). For $K_1 = 2.5$ it will be $\phi < 0.6435$ only one fixed point will exist and that will be stable, so we only get the second-order transition in this range. when $\phi > 0.6435$ two nontrivial fixed points one stable and the other unstable exists which gives bistability in this region along with a trivial stable fixed point. For fixed K_2 and varying K_1 with different ϕ we have to study bifurcation diagrams to check when the trivial case for r=0 will become unstable via subcritical pitchfork bifurcation and nontrivial branch becomes stable via saddle-node bifurcation so to check these we need to see it from numerical simulations. This work is recently done by a different group and we were also doing this same model parallelly and so they have done this before and have discussed it in detail in their arxiv preprint[11] and for the time being we are not putting the numerical simulations.

We see here that there is a synchronization transition from abrupt to continuous for a

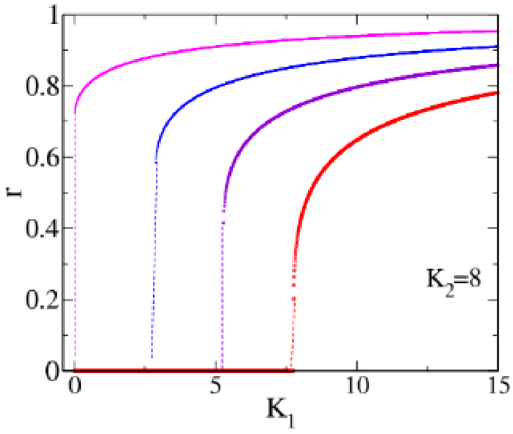

FIGURE 5.1: r vs K_1 for fixed K_2=8

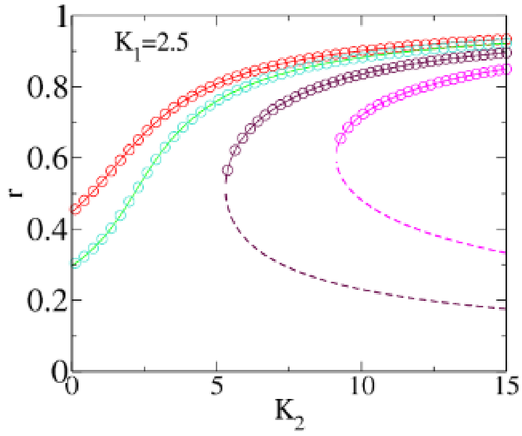

FIGURE 5.2: r vs K_2 where $K_1 = 2.5$

fixed value of K_2 and varying ϕ with increasing K_1 and in the second figure complete opposite observation is made in which there is a continuous to abrupt transition for fixed K_1 and varying ϕ with increasing K_2. Here on including pairwise coupling with phase lag parameter, we see that on varying ϕ nature of the transition is changed and this introduction of ϕ can be proved to be very useful in many applications whenever we want to change the nature of transition according to our needs.

5.2 Summary

We have studied here how the phase lag parameter affects and alter the collective dynamics of the system by introducing the phase lag parameter beyond pairwise in 2-simplicial complexes by changing the transition point by causing frustration in the system and also changing the type of transition.

5.2.1 Outlook

The pairwise term can also be added in the $2\theta_i$ model to see if there are any interesting phenomena that can take place.This model can further be generalized by introducing inertia along with phase lag which may give rise to a new phenomenon.

Bibliography

[1] Hidetsugu Sakaguchi and Yoshiki Kuramoto. "A Soluble Active Rotater Model Showing Phase Transitions via Mutual Entertainment". In: *Progress of Theoretical Physics* 76.3 (Sept. 1986), pp. 576–581. ISSN: 0033-068X. DOI: 10.1143/PTP.76.576. eprint: https://academic.oup.com/ptp/article-pdf/76/3/576/5302137/76-3-576.pdf. URL: https://doi.org/10.1143/PTP.76.576.

[2] Steven H. Strogatz. "From Kuramoto to Crawford: exploring the onset of synchronization in populations of coupled oscillators". In: *Physica D Nonlinear Phenomena* 143.1-4 (Sept. 2000), pp. 1–20. DOI: 10.1016/S0167-2789(00)00094-4.

[3] Diego Pazó. "Thermodynamic limit of the first-order phase transition in the Kuramoto model". In: *Phys. Rev. E* 72 (4 Oct. 2005), p. 046211. DOI: 10.1103/PhysRevE.72.046211. URL: https://link.aps.org/doi/10.1103/PhysRevE.72.046211.

[4] Edward Ott and Thomas M. Antonsen. "Low dimensional behavior of large systems of globally coupled oscillators". In: *Chaos: An Interdisciplinary Journal of Nonlinear Science* 18.3 (Sept. 2008). 037113. ISSN: 1054-1500. DOI: 10.1063/1.2930766. eprint: https://pubs.aip.org/aip/cha/article-pdf/doi/10.1063/1.2930766/13857986/037113_1_online.pdf. URL: https://doi.org/10.1063/1.2930766.

[5] Seth A. Marvel, Renato E. Mirollo, and Steven H. Strogatz. "Identical phase oscillators with global sinusoidal coupling evolve by Möbius group action". In: *Chaos: An Interdisciplinary Journal of Nonlinear Science* 19.4 (Oct. 2009). 043104. ISSN: 1054-1500. DOI: 10.1063/1.3247089. eprint: https://pubs.aip.org/aip/cha/article-pdf/doi/10.1063/1.3247089/13277393/043104_1_online.pdf. URL: https://doi.org/10.1063/1.3247089.

[6] Edward Ott and Thomas M. Antonsen. "Long time evolution of phase oscillator systems". In: *Chaos: An Interdisciplinary Journal of Nonlinear Science* 19.2 (May 2009). 023117. ISSN: 1054-1500. DOI: 10.1063/1.3136851. eprint: https://pubs.aip.org/aip/cha/article-pdf/doi/10.1063/1.3136851/16693913/023117_1_online.pdf. URL: https://doi.org/10.1063/1.3136851.

[7] Albert-László Barabási. "Network science". In: *Philosophical Transactions of the Royal Society A: Mathematical, Physical and Engineering Sciences* 371.1987 (2013), p. 20120375. DOI: 10.1098/rsta.2012.0375. eprint: https://royalsocietypublishing.org/doi/pdf/10.1098/rsta.2012.0375. URL: https://royalsocietypublishing.org/doi/abs/10.1098/rsta.2012.0375.

[8] James Ladyman, James Lambert, and Karoline Wiesner. "What is a complex system?" In: *European Journal for Philosophy of Science* 3 (June 2013). DOI: 10.1007/s13194-012-0056-8.

[9] Per Sebastian Skardal and Alex Arenas. "Abrupt Desynchronization and Extensive Multistability in Globally Coupled Oscillator Simplexes". In: *Phys. Rev. Lett.* 122 (24 June 2019), p. 248301. DOI: 10.1103/PhysRevLett.122.248301. URL: https://link.aps.org/doi/10.1103/PhysRevLett.122.248301.

[10] Per Sebastian Skardal and Alex Arenas. "Higher order interactions in complex networks of phase oscillators promote abrupt synchronization switching". In: *Communications Physics* 3.1 (2020), p. 218.

[11] Sangita Dutta et al. *Impact of phase lag on synchronization in frustrated Kuramoto model with higher-order interactions*. 2023. arXiv: 2305.01706 [nlin.AO].